Proceedings of the World Congress on Electrical Engineering and Computer Systems and Science (EECSS 2015)
Barcelona, Spain – July 13 - 14, 2015
Paper No. 336

Defect Detection Based on the Variance of the Surface Normal Direction Using a Ring-Lighting System

Yoshiharu Nakamura
Mitsui High Tech, Inc.
12-10-1, Komine, Yahatanishi, Kitakyusyu, Fukuoka, 807-8588 Japan
yoshiharu-nakamura@mitsui-high-tec.com

Shuichi Enokida
School of Computer Science and Systems Engineering, Kyushu Institute of Technology
Kawadu, Izuka, Fukuoka, 820-8502 Japan
enokida@ai.kyutech.ac.jp

Abstract- Recently, demand has grown for defect detection processes utilizing machine vision applications. In our studies, we are particularly interested in the IC lead frames used when making semiconductor products. In previous work, we proposed a detection method that assumes the variance in the intensity of oriented gradients in images that include defective areas will be larger than that found in acceptable areas. In this paper, another defect detection method is proposed for detecting different defect types. This method assumes that the variance of the surface normal direction in a local area that includes defects will be large. However, while this method achieved some good experimental results, a number of disadvantages were encountered. One of these is that it is difficult to decide the parameters, the size of the region of interest, weight values, and other factors.

***Keywords*:** machine vision, multiple light source imaging, defect detection, IC lead frame

1. Introduction

In semiconductor product defect detection processes, machine vision applications based on pattern matching methods are most commonly used. However, in the case of the numerous lines engraved on IC lead frames used for mounting semiconductor components, it is difficult to determine exact line positions due to parallelism problems related to the IC lead frame itself. This makes it difficult for matching processes to deal with the partial shifts that result from individual variations. Therefore, a defect detection method that does not rely on pattern matching between a template image and test input images is needed.

Recently, demand has arisen for defect detection processes that utilize machine vision applications. This is especially needful for the abovementioned IC lead frames used in semiconductor manufacture, which require both high quality and miniaturization.

However, when conventional image processing methods are used for verifying various defects, constant adjustments must be made in order to maintain a balance between the detection size, the kind of defect sought, and the error detection processes. Ultimately, this means it is necessary for a human being to review and confirm the identification results.

Therefore, there is a tendency to detect defects that has large variance in the local image without a temporal image of good condition [1]. Our previously proposed method assumes that the variance in the intensity of oriented gradients in local images that include defect areas will be larger than that found in the acceptable areas [2]. In this paper, another method is proposed for detecting different types of defects.

This method assumes that the variance of the surface normal direction in the area that includes defects will be large.

Our method uses two variance types to determine whether or not defects exist. The first variance is calculated by using multiple images that are acquired while varying the light source direction. This value is used to determine whether or not the normal direction at the point (or small region) of interest is parallel to a camera's optical axis. However, since this assessment is unsatisfactory in situations where the stage has the slightest tilt with respect to the optical axis, an additional assessment value is needed.

The second value is calculated by using the maximum value of the variance. These values are calculated in each image acquired from several light source directions. The second value is capable of discriminating between flat and curved areas at the surface of the region of interest. Finally, the weighted sum of these two values is utilized to identify defects. In Section 2, the relationships between the surface normal direction and reflected light are explained. Our newly proposed method is described in Section 3, after which experimental results are shown in Section 4.

2. Relations of Surface Normal Direction and Reflected Light

2. 1. Proposed Method Viewpoint

The state of light reflected from an object surface has been represented in a variety of reflection models (Fig. 1). In many such reflection models, light values are approximated by the sum of the specular and diffuse reflection components [3].

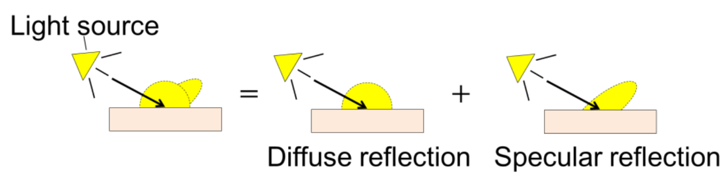

Fig. 1. Diffuse and specular reflection components.

Lambert models are used as a diffusion reflection model at viewing point X of the object surface. In Eq. (1), it is assumed that the Lambert model is proportional to the cosine of the angle defined by the normal direction $\boldsymbol{N}$ and the direction of the light source $\boldsymbol{L}$ (Fig. 2).

$$i = \rho_d \max(0, \boldsymbol{N} \cdot \boldsymbol{L}) \tag{1}$$

ρ_d is diffuse reflectance.

Additionally, in Eq. (2), the Phong model [4], which is a specular reflection model, is approximated as a power of the cosine of the angle α defined by the viewing direction $\boldsymbol{V}$ and specular reflection $\boldsymbol{L'}$.

$$i = \rho_s \cos^n \alpha \tag{2}$$

Where ρ_s is specular reflectance and n is a parameter representing the surface roughness.

The intensity of reflected light depends on the surface normal direction in both the diffuse reflection component (represented by Lambert model) and the specular reflection component (represented by Phong model).

If the viewing direction is parallel to the surface normal direction, as illustrated on the left side of Fig. 3, the reflected light intensity does not change when the light source direction rotates around the viewing direction. However, when the viewing direction is not a parallel to the surface normal direction, the reflected light intensity will vary as the light source rotates around the viewing direction.

Therefore, by obtaining and analyzing multiple images while the light source direction is rotated around the viewing direction, it is able to determine whether the viewing direction is parallel to the surface normal direction.

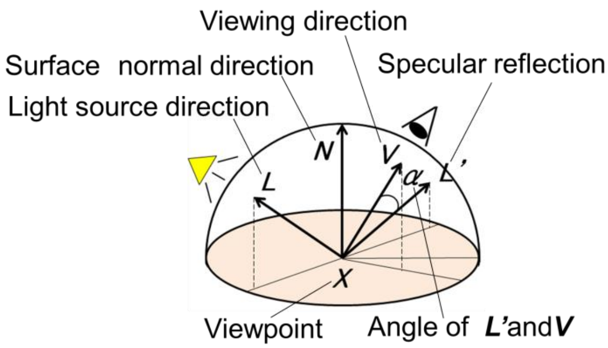

Fig. 2. Angle parameters and vectors used for a reflection model.

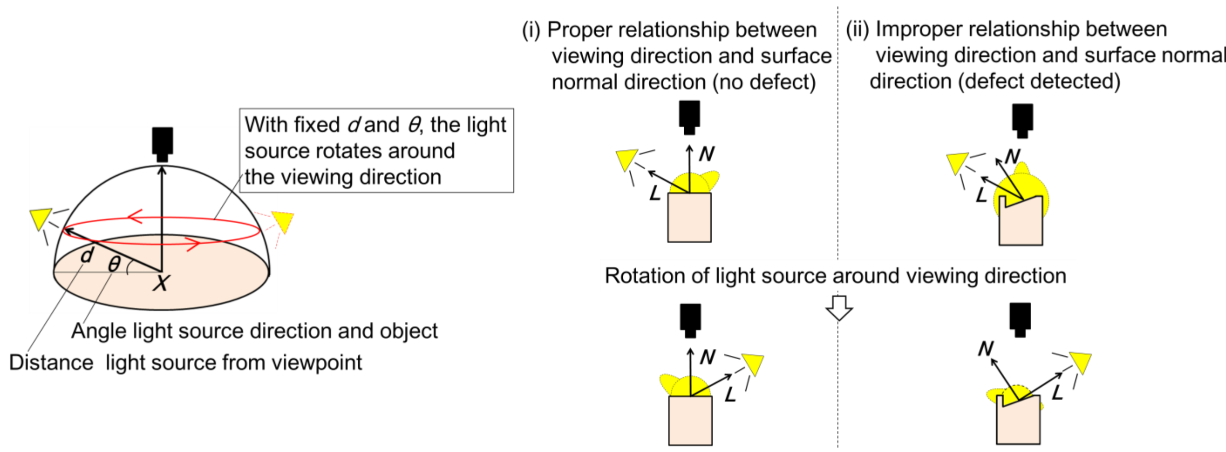

Fig. 3. Light source and surface normal direction.

In this paper, we propose a detection method that is capable of detecting several defect types using only one model and parameter setting. This proposed method assumes that the variance in the surface normal direction in the local area that includes the defects is large. The surface normal directions for such defects are shown in Fig. 4.

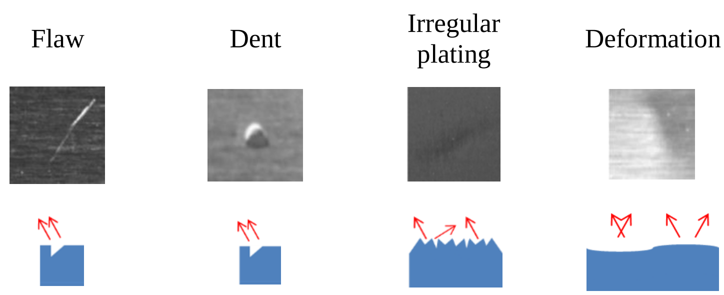

Fig. 4. Defects and surface normal direction.

3. Detection Method

In our method, two variances are utilized to determine whether or not a defect exists. Each variance is calculated by using multiple images acquired by varying the light source direction.

3. 1. The Variance Value V_d (Direction Changes)

The first variance V_d is calculated in the same block by using multiple images which are acquired by varying the N ($i = 1, 2 \cdot \cdot \cdot N$) direction of the light source (Fig. 5). (w_d : width size of the block, h_d : height size of the block)

$$V_d(x,y) = \frac{1}{N \cdot w_d \cdot h_d} \sum_{i=1}^{N} \sum_{x=1}^{w_d} \sum_{y=1}^{h_d} (I_{i,x,y} - \bar{I_d})^2 \tag{3}$$

$\bar{I_d}$ is the mean in the block

A raster scan of the inspection area is performed and V_d is then computed for all the pixels using Eq. (3).

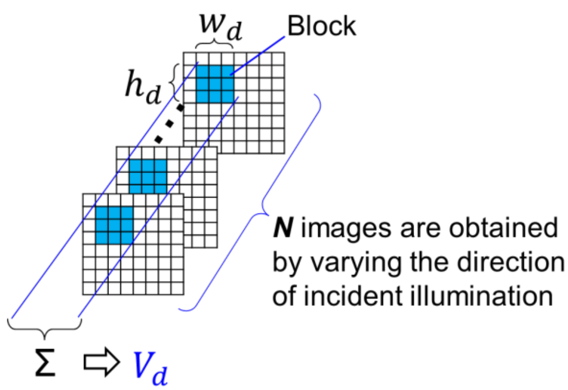

Fig. 5. V_d calculation method.

This value is used to determine whether or not the normal direction at the point (or small region) of interest is parallel to the camera's optical axis. However, this assessment alone is inadequate when the stage has the slightest tilt with respect to the optical axis. Therefore, a second assessment value is needed to overcome this problem (Fig. 6).

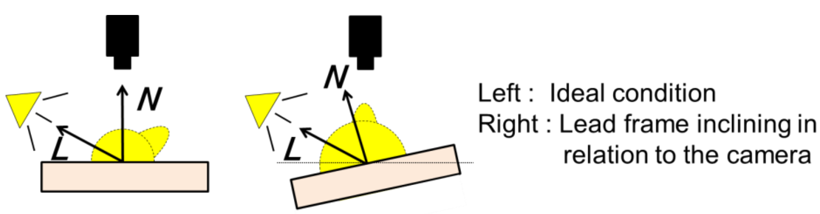

Fig. 6. Proper and improper optical system alignment.

3. 2. The Variance Value V_r (Peripheral Area)

The second value V_r is calculated by using the maximum of the measured variance values. These values are calculated for images acquired from several light source directions, respectively (Fig. 7) (w_r: block width size, h_r: block height size).

$$V_r^{(i)}(x,y) = \frac{1}{w_r \cdot h_r} \sum_{x=1}^{w_r} \sum_{y=1}^{h_r} (I_{x,y} - \bar{I_r})^2 \tag{4}$$

$$V_r(x,y) = \max_{i \in N} \{V_r^{(i)}(x,y)\}$$

$\bar{I_r}$ is the mean in the block

A raster scan of the inspection area is performed and V_r is computed for all pixels using Eq. (4).

Because this value is capable of discriminating between flat and curved areas at the (large) surface region of interest, it overcomes the problem that results when the stage is tilted with respect to the optical axis. However, its use is insufficient when the defect size is bigger than the block size because a variance value sufficient for detection cannot be acquired. Therefore, it is necessary to carefully estimate the defect size when setting up the block size. Additionally, if a light source direction does not permit the acquisition of a brightness value that shows a difference between peripheral and defective areas, a satisfactory variance value will not be acquired. Therefore, it is necessary to prepare and utilize numerous light source directions. (V_d is expected to be a number of light sources less than the V_r.)

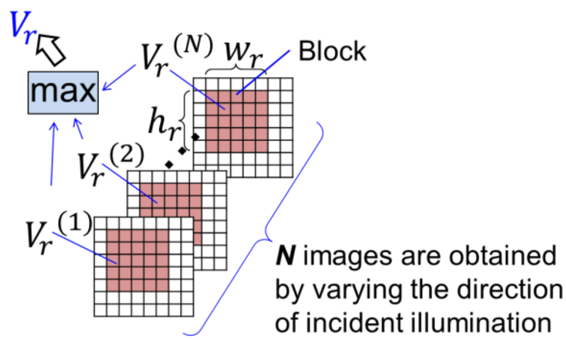

Fig. 7. V_r calculation method.

3. 3. Unification of V_d and V_r

Finally, the weighted sum of these two values is utilized to detect defects.

The block size used for V_d and V_r that sets up to become $w_r > w_d$ and $h_r > h_d$, because V_d is calculated in a small region, and V_r is calculated in a large region, as shown in Fig. 8.

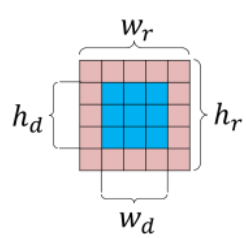

Fig. 8. Relations of w_r, w_d, h_r, and h_d.

V_d and V_r are normalized at each maximum. Defect detection is then performed using α, which determines the rate of V_d value and V_r value, and Th, which determines a detection level.

$$(1-\alpha)\frac{V_d(x,y)}{\max V_d}+\alpha\frac{V_r(x,y)}{\max V_r} > Th \tag{5}$$

4. Experimental Results

4. 1. Experimental Environment

Fig. 9 shows the experimental environment used to acquire images. We rotated the light emitting diode (LED) ring-lighting which opened at 45° by 22.5° increments in order to acquire 16 images while varying the direction of incident illumination.

The brightness distribution when the lighting is placed on the right side of a white paper, as shown in Fig. 9, is so close to a light source that the light volume near the center is only becomes stabilized when the illumination direction is rotated. However, since it is a basic experiment conducted simply to verify the validity of this method, only the area near the center of the camera view, where light volume was stabilized, was used in this study.

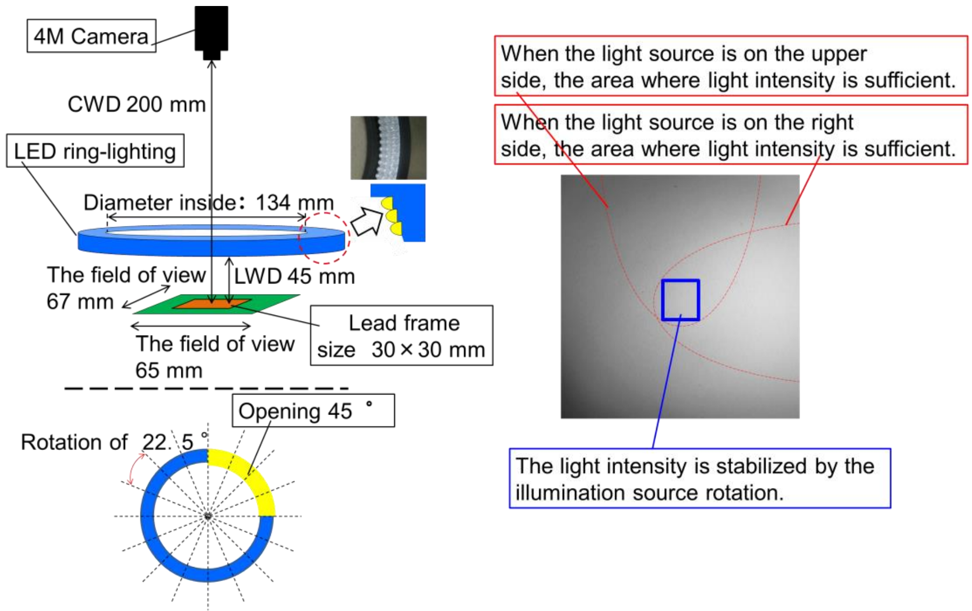

Fig. 9. Imaging environment and brightness distribution.

4. 2. Experimental Method

The defects (dent, irregular plating, and deformation) examined in our experiments are shown in Fig. 4. Fig. 10 shows an example of an IC lead frame that has a flaw in the center. Each defect is located in the center of the view, because it was where the light volume was stabilized in relation to the center of the camera view when the light source was rotated. Multiple images of each defect were acquired from the 16 light source directions. Defect detection accuracies were then measured in several block sizes (w_d, h_d, w_r, and h_r), α, and *Th*.

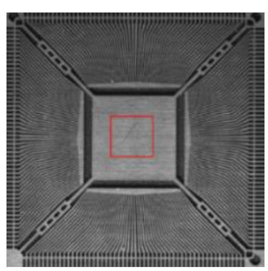

Fig. 10. IC lead frame with a flaw.

4. 3. Experimental Method

When IC lead frames are inspected automatically, false defect detections often occur. Of course, our proposal method may also result in false detections if the parameters are set in an arbitrary manner, as shown in Fig. 11. Since frequent false detection occurrences are troublesome, a countermeasure for reducing overdetection is needed.

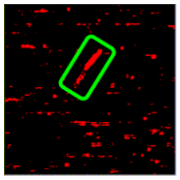

Green square
Inside: Appropriate detection
Outside box: False detection

Fig. 11. Error detection.

4. 4. Experiment

Block sizes (w_d, h_d for V_d calculation. w_r, h_r for V_r calculation) were appropriately examined via experiment, $w_d = h_d = 5$ $w_r = h_r = 25$. The region described as "appropriate detection" is the area where actual defects have been detected and where false detections does not occur. The "appropriate detection" parameter setting for all defects is shown in Fig. 12.

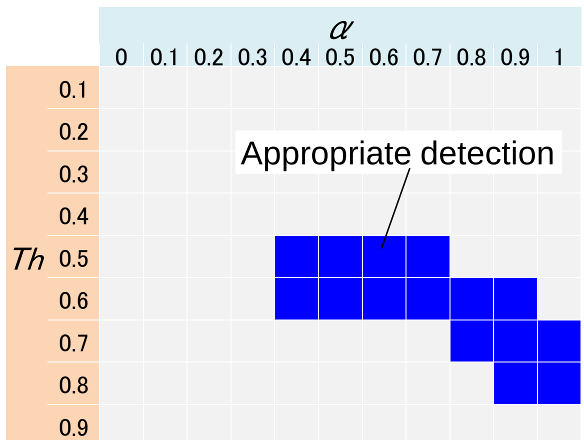

Fig. 12. Parameter setting that is effective for all defects

"Appropriate detection" parameters also exist for irregular plating and deformation related defects. However, since neither irregular plating nor deformations have strong edges, detection is difficult when using the conventional methods discussed earlier.

Using our proposed method, we checked for "appropriate detection" using the same defect parameter shown in Fig. 12 (for all other defects), and were able to confirm its effectiveness. The detection result of $\alpha = 0.5$, $Th = 0.5$ is shown in Fig. 13. However, when the value of α is 0.4 or more, the "appropriate detection" region appears. The "appropriate detection" region also appears at the time of $\alpha = 1.0$ (V_d is not used). We considered three reasons why these phenomena occurred:

I. V_r is effective when the block size is larger than the defect, as described in Section 3.2. Since an appropriate block size was chosen for the experiments in this research, the value of V_r might have become dominant.
II. Since the light source provided illumination from 16 directions, it is thought that there was a light source direction that provided enough of a distribution value to allow the defect area to be acquired from an image of one sheet.
III. When the optical system is in an ideal state, V_d is effective. These optical conditions may have appeared as inclinations.

In this research, our proposal method achieved a good performance, when the value of V_r is large. When a situation occurs where the defect size is an unknown and light source directions are reduced, the value of V_d is expected to become large.

By using the appropriate parameter setting (α = 0.8, Th = 0.6) for defect detection which is obtained by pre-experiment, our proposal method achieved 90% success rate on other 20 defects example images. Examples of appropriate detection results are shown on the left side of Fig.14. In addition, two false detection results are shown on the right side of Fig.14. About false #1, it is thought that the inspection area size (w, h) was not appropriate to detect that large defect. About false #2, it is thought that the whole of defect was not detected due to inappropriate normalization in Eq. (5) with a few high values of V_r and/or V_d.

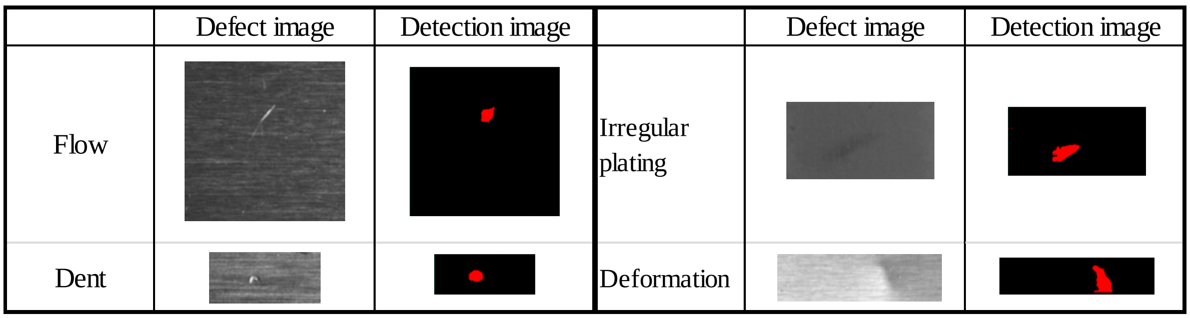

Fig. 13. Detection images (α=0.5 Th=0.5).

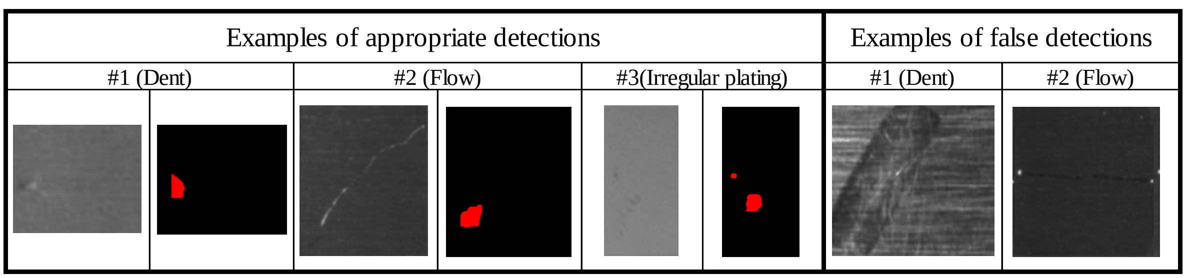

Fig. 14. Examples of detections (α=0.8 Th=0.6).

5. Conclusion

Using our proposal method, variations in the normal direction of a defective area can be observed. This method calculates the distribution value between multiple images that are acquired by varying the direction of incident illumination. In experiments using our proposed method, we showed it was possible to detect defects that were previously difficult to identify using conventional methods.

As a future problem, when applying this method to an entire IC lead frame, it is expected that error detection problems will occur in the corners of the design because of the large normal direction distribution values. This will make it necessary to examine masking processes or parameter adjustments that take corners and edges into consideration. In addition, while we intend to discover and use appropriate parameters via experiments, it would be optimal if a method could be developed to produce parameters that are self-adjusting.

References

Aoki, K., Funahashi, T., Koshimizu, H., & Miwata, Y. (2013). KIZUKI' Algorithm Inspired by Peripheral Vision and Involuntary Eye Movement. *J. of the Japan Soc. for Precision Eng.*, *79*(11), 1045-1049.

Nakamura, Y., Masuzoe, M., & Enokida, S. (2013). Study of Defect Verification based on Histogram of Oriented Gradients in Local Area. *The Inst. of Image Electron. Engineers of Japan, 264th Study Meeting*.

Mukaigawa, Y. (2010). Measurement and Modeling of Reflection and Scattering. *IPSJ SIG Tech. Rep.*, *172*(34).

Phong. B. T. (1975). Illumination for Computer Generated Pictures. *Proc. SIGGRAPH'75*, 311-317.

Woodham, R. J. (1980). Photometric Method for Determining Sur-Face Orientations from Multiple Images. *Optical Eng.*, *19*, 139-144.

Ikehata, S., Aizawa, K. (2014). Photometric Stereo using Con-strained Bivariate Regression for General Isotropic Surface. *IEEE Trans. on Pattern Anal. and Mach. Intell.*